Supporting Information

Prahlad and Morimoto 10.1073/pnas.1106557108

SI Materials and Methods

***C. elegans* Strains and Growth Conditions.** The following *C. elegans* strains were used: Bristol WT N2, *gcy-8* (*oy44*) IV, OH161 *ttx-3* (*oh161*) X, CX10 *osm-9*(*ky10*) IV, CX4544 *ocr-2* (*ak47*) IV, CB1402 *unc-15*(*e1402*)I, AM140 rmIs132[P(*unc-54*) Q35::YFP], GF80 dgEx80[pAMS66 *vha-6*p::Q44::YFP + rol-6(su1006) + pBluescript II], SOD-1 G93A: [P(*unc-54*) SOD-1^{G93A}::YFP], EG3404 *unc-31*(*e928*) IV.

gcy-8 (*oy44*) were obtained from I. Mori (Nagoya University, Nagoya, Japan). *unc-31*(*e928*) were obtained from Janet Richmond (University of Illinois at Chicago, Chicago, IL). The remaining strains were obtained from the *Caenorhabditis* Genetics Center or frozen worm stocks from our laboratory. The *vha-6*p::Q44::YFP + *rol-6*(su1006) in the GF80 strain was integrated and backcrossed three times before use. To generate *gcy-8* and *ttx-3* mutant animals expressing Q35, Q44 or *unc-15* (ts), *gcy-8* (*oy44*) IV or *ttx-3*(*ks5*) X animals were crossed and the F2 progeny selected for YFP expression, or the temperature-sensitive phenotype, and their genotypes verified by PCR when necessary. To generate the *gcy-8* (*oy44*); *unc-31*; Q35 or *gcy-8* (*oy44*); *unc-31*; Q44 animals, *gcy-8* (*oy44*); *Q35*/+ *or gcy-8* (*oy44*); *Q44*/+ males were crossed to *unc-31* hermaphrodites. As *gcy-8* and *unc-31* are on the same chromosome, 400 F2 were singled and recombinant homozygotes selected as those that transmitted 100% fluorescent progeny, showed the *unc-31* phenotype, and were homozygous for *gcy-8* as determined by PCR.

The following *gcy-8* (*oy44*) IV primers were used for genotyping: gcy8 within F1, 5′-GGA AAA ACT GGT CGC TGA-3′; gcy8 within R1, 5′-GCT AGT CGG AAA CCC AGA-3′; gcy8 flanking F1, 5′-CAT GCT TCC CAG ATT GGA-3′; gcy8 flanking R1, 5′-CTC TGC AAT CCT GTT GGA-3′.

The bacteria Op50 was used for feeding *C. elegans* (1). Standard NGM plates (1) 6 cm in diameter were used. Plates were seeded with 200 to 500 μL of an overnight culture of Op50 grown in Luria–Bertani broth. The bacteria were allowed to establish a dense bacterial lawn at room temperature for 2 to 4 d before being plated with the appropriate *C. elegans* strains. Care was taken to prevent contamination with other bacteria.

Populations were maintained by placing 10 animals in L4 stage on Op50 seeded plates, allowing them to reproduce at 20 °C, or in the case of *unc-15*(ts), *gcy-8*;*unc-15*(ts), or *ttx-3*;*unc-15*(ts) animals, at 15 °C, and selecting L4 progeny after 48 to 78 h to be transferred onto new, similarly seeded NGM plates at the respective temperatures for use in experiments. Three such plates constituted one sample in an experiment, and were scored for aggregation phenotypes or used to assay mRNA levels. Sufficient *n* values were obtained by increasing the number of plates, and not by increasing the number of animals per plate.

RNA Extraction and Quantitative RT-PCR. Ten to 20 adult animals were picked from the control or experimental plates into 10 μL of nuclease-free water (catalog no. AM9938; Ambion) and snap-frozen in liquid nitrogen. The samples were thawed, suspended in 200 μL of TRIzol reagent (catalog no. 15596–026; Invitrogen), and vortexed for at 4 °C for 20 min. Chloroform (50 μL) was added to extract RNA. The samples were allowed to stand at room temperature for 5 min and centrifuged at 14,000 rpm (Eppendorf Centrifuge 5417C, Rotor #F45-30-11) for 15 min, and then 125 μL of the aqueous layer was transferred to a new tube. The nucleic acids were precipitated using an equal volume of iso-amyl alcohol, centrifuged at 14,000 rpm (Eppendorf Centrifuge 5417C, Rotor # F45-30-11) for 15 min, washed using 70% ethanol, and dried. The RNA was resuspended in 10 μL water, and heated for 5 min at 60 °C to dissolve the RNA. The DNA-free Kit (catalog no. 1906; Ambion) was used to digest the contaminating DNA according to the manufacturer's instructions. mRNA was then reverse-transcribed by using the iScript cDNA Synthesis Kit (catalog no. 170–8891; Bio-Rad). Quantitative PCR was performed using iQ SYBR Green Supermix (catalog no. 170–8880; Bio-Rad) in the iCycler system (Bio-Rad) at a 25-μL sample volume, in thin-walled 200-μL PCR plates (catalog no. 223–9441) sealed with optical quality sealing tape (catalog no. 223–9444).

Relative amounts of *hsp* mRNA were determined using the comparative C_T method for relative quantitation (2). The quantification of *hsp* mRNA levels within an experiment were relative to actin mRNA that was used as an internal control. The primers used were determined to be of comparable efficiency in amplifying a range of dilutions of cDNA. The range of input of RNA was determined by using serial dilutions of cDNA. Concentrations that yielded a C_T value lower than 30 for both the target cDNA and actin was used in all experiments. This typically corresponded to 1 μL of the total cDNA obtained per sample. C_T values were obtained in triplicate for each sample (technical triplicate), and three samples were used per experiment. Each experiment was then repeated a minimum of three times. All relative changes of *hsp* mRNA in the mutant strains were normalized to WT values except where otherwise noted. SDs were calculated by using the delta(delta C_T) values from multiple repetitions, when the data were normalized to the delta C_T value of one WT (N2) from an experiment, arbitrarily chosen. This normalization allowed us to get a better estimate of the variability across biological samples.

The primers used for the PCR analysis were:

hsp70 (C12C8.1), forward, 5′-ACT CAT GTG TCG GTA TTT ATC-3′; reverse, 5′-ACG GGC TTT CCT TGT TTT-3′. *hsp70* (F44E5.4), forward, 5′-AAT GAA CCA ACT GCT GCT GCT CTT-3′; reverse, 5′-TGT CCT TTC CGG TCT TCC TTT TG-3′. hsp16.2, forward, 5′-ACT TTA CCA CTA TTT CCG TCC AGC-3′; reverse, 5′-CCT TGA ACC GCT TCT TTC TTT G-3′; actin, forward, 5′-ATC ACC GCT CTT GCC CCA TC-3′; reverse, 5′-GGC CGG ACT CGT CGT ATT CTT G-3′. hsp-1, forward, 5′-CTC GAG TCA TAC GCC TTC AAC CTT A-3′; reverse, 5′-GGC CAA TCC TTC CAA ATC CTT CTG-3′. YFP, forward, 5′-GGTGGCATCGCCCTCGCCCTCGCCG-3′; reverse, 5′-ATGGTGAGCAAGGGCGAGGAGCTGTTC-3′. hsp90 (daf-21), forward, 5′-CGC TAC CAG GCA CTC ACC GAG-3′; reverse, 5′-GGA CAA GCT CTT GTA GAA CTC AG-3′. *hsp70* (C30C11.4), forward, 5′-GAT GCC CCC GTT GTC TTC A-3′; reverse, 5′-GGC TGG GGC TCT TCC TTC TT-3′.

RNAi Experiments. *Escherichia coli* strain HT115 (DE3) harboring the appropriate dsRNA expressing plasmid from the genomic RNAi library (Source BioScience/Geneservice) were grown overnight in Luria–Bertani broth containing ampicillin (100 μg/mL) and tetracycline (12.5 μg/mL). Bacteria (200–500 μL) were seeded onto NGM plates containing ampicillin (100 μg/mL), tetracycline (12.5 μg/mL), and 0.5 mM isopropyl β-d-thiogalactosidase. Care was taken to ensure that the plates grew a healthy lawn of RNAi bacteria by allowing the bacteria to grow for 2 to 4 d before use. RNAi constructs used were *hsf-1*, *daf-16*, *hsp70* (C12C8.1), and *hsp90* (daf-21), *gcy-8*, *gcy-23*, *nhr-38*, and *ceh-10*. *E. coli* strain HT115 (DE3) expressing the RNAi plasmid vector L4440 alone was used as the control. In all cases, 10

to 20 L4 larvae were placed on RNAi plates, and experiments were repeated a minimum of three times.

Motility Assays. The motility of N2, *gcy-8*, Q35, *gcy-8*;*Q35*, *ttx-3*;*Q35*, *unc-15*(ts), *gcy-8*;*unc-15*(ts), *ttx-3*;*unc-15*(ts) were recorded upon transferring 10 animals to a new 6-cm plate seeded uniformly with Op50 equilibrated to room temperature. Movies of crawling animals were recorded with a Leica MZ10 microscope and Hamamatsu C10600-10B (Orca-R2) camera by using SimplePCI software (Leica) at 2 × 2 binning and 5 frames/s, and analyzed by using ImageJ. Movie cxd files were imported directly into ImageJ (3) using the LOCI bio-formats plug-in (http://www.loci.wisc.edu/bio-formats/imagej), and flickering from 60-Hz light source was removed by normalizing average intensity from each frame using a custom stack deflicker plug-in. Animals were enhanced for visual analysis by calculating the difference between each frame, and the constant background calculated using Maximum Z stack projection, resulting in movies that were converted to binary format using Otsu thresholding (4). Binary objects representing the animals were tracked by using a custom ImageJ plug-in based on MTrack2 (5) by Nico Stuurman. The average speed of animal was calculated by dividing the length by the duration of each track. Each sample of 10 animals was measured only once. At least three samples of 10 animals was considered one biological sample, and each report of motility involved three to five biological samples.

FRAP. We examined the state of the polyQ aggregates by using FRAP. The methods used were as previously described (6). Specifically, to examine whether YFP foci corresponded to soluble or immobile aggregates, 2- to 4-d adult animals expressing polyQ in the intestine (Q44, *gcy-8*;*Q44*, *ttx-3*;*Q44*; *unc-31:Q44*), or in muscle cells (Q35 *gcy-8*;*Q35*, *ttx-3*;*Q35*; *unc-31*;*Q35*), were immobilized and 10 to 30 polyQ::YFP foci in each strain were bleached and their recovery monitored over a duration of 1 min. Whenever possible, similar anatomical regions were chosen for bleaching in the WT and mutant animals. Thus, for Q44 expressing animals, foci in the first cell of the intestine were consistently chosen. This was not always possible for the *gcy-8*; *Q44* animals, as they contained such few aggregates, and in this case, any of the few other foci present within the animal were picked. For determining the status of Q35 protein in the muscle cells, foci in the head region and body wall muscle cells near the vulva were consistently chosen. Only a maximum of two areas were bleached within any one animal. To determine whether the areas of diffuse fluorescence seen in the thermosensory mutant animals corresponded to freely diffusing polyQ::YFP protein, approximately 20 such regions in each of the stains were also exposed to a similar regimen, and fluorescence intensity was monitored over time. In all strains, the brightest regions of diffuse fluorescence were chosen for bleaching. In the *gcy-8*; Q44 and *unc-31*:Q44 animals, these corresponded to nuclei containing diffuse Q44::YFP protein. Soluble YFP expressed in body wall muscle cells was used as the control. Imaging was conducted at the same magnification for all animals at 0.1% power of a 514-nm laser, and bleaching was conducted by the 514-nm laser focused onto a defined area for 10 iterations at 100% power. Relative fluorescence intensity was determined as $(T_t / C_t) / (T_0 / C_0)$, with T_0 representing the total intensity of the region of interest before photobleaching and T_t the intensity in the same area at any time after. The signal was normalized against an unbleached area in the same aggregate. C_0 is a control area before bleaching and C_t represents any time after bleaching.

SDS/PAGE Gels and Western Blots for Examining Protein Levels. A monoclonal mouse anti-polyglutamine antibody (catalog no. P1874; Sigma) was used to detect polyQ expression, and a monoclonal anti–α-tubulin antibody (catalog no. I-5168, clone B-5-1-2; Sigma) was used to detect tubulin. IR-conjugated secondary goat anti-mouse IR 680 (Alexa Fluor catalog no. P1874) and sheep anti-mouse IR 800 IgG (catalog no. 610–632-002; Rockland Immunochemicals) were used as secondary antibodies. The membranes were probed sequentially with each of the primary antibodies and scanned using a LI-COR Odyssey fluorescent imager at 700 nm and 800 nm, and the molecular weights of the proteins were determined against Dual Color Precision Plus Protein Standards (catalog no. 161–0374; Bio-Rad). An anti-GFP IR 800 antibody (catalog no. 600–132-215; Rockland Immunochemicals) was also used to ascertain that there was no cleavage of YFP from the polyQ-expressing polypeptide.

Statistical Methods. In all cases, paired, two-tailed Student *t* tests were used to assess significance. A *P* value lower than 0.01 was considered significant. For the determination of changes in the number of aggregates, the average numbers of aggregates in the mutant animals (*gcy-8*;*Q44*, *ttx-3*;*Q44*; *osm-9*; *Q44*, *ocr-2*; *Q44*, *unc-31:Q44*, *gcy-8*;*Q35*, *ttx-3*;*Q35*; *unc-31*;*Q35*; *osm-9*; *Q35*, *ocr-2*; *Q35*) in each biological sample of 20 animals was compared with that in the WT animals (*Q35*, *Q44*) of comparable ages. For assessing the significance of changes in motility, and numbers of larvae, data from each of the mutant strains was compared with that from WT animals of comparable age. For the RNAi experiments, the data (e.g., number of aggregates, relative *hsp70* C12C8.1 mRNA levels) from exposure to the experimental RNAi was compared with data of the same strain exposed to control RNAi. No tests were conducted if the data differed obviously, and by more than two SDs.

1. Brenner S (1974) The genetics of Caenorhabditis elegans. *Genetics* 77:71–94.
2. Applied Biosystems (2004) *Guide to Performing Relative Quantitation of Gene expression using Real-Time Quantitative PCR.* Available at http://www.appliedbiosystems.com/support/apptech/. Accessed January 12, 2010.
3. Collins TJ (2007) ImageJ for microscopy. *Biotechniques* 43(suppl 1):25–30.
4. Otsu N (1979) A threshold selection method from gray-level histograms. *IEEE Trans Syst Man Cybernet* 9:62–66.
5. Klopfenstein DR, Vale RD (2004) The lipid binding pleckstrin homology domain in UNC-104 kinesin is necessary for synaptic vesicle transport in Caenorhabditis elegans. *Mol Biol Cell* 15:3729–3739.
6. Brignull HR, Moore FE, Tang SJ, Morimoto RI (2006) Polyglutamine proteins at the pathogenic threshold display neuron-specific aggregation in a pan-neuronal *Caenorhabditis elegans* model. *J Neurosci* 26(29):7597–7606.

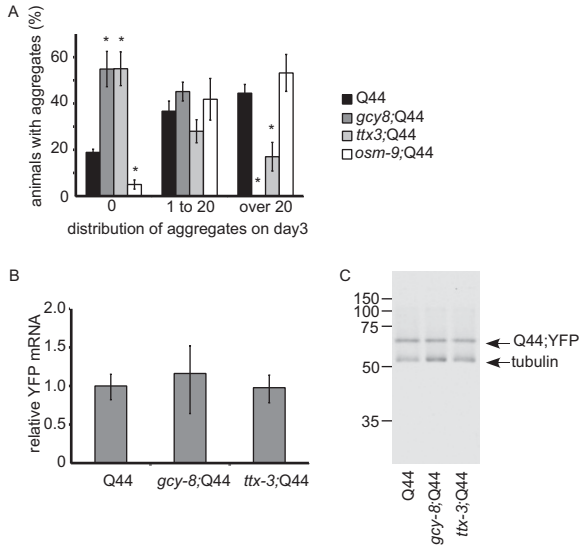

Fig. S1. Thermosensory neurons regulate the aggregation of Q44 in *C. elegans* intestine. (*A*) Percentage of Q44, *gcy-8*;*Q44* and *ttx-3*;*Q44* and *osm-9*; Q44 day 3 adult animals that contain 0, between one and 20, and more than 20 aggregates. Error bars indicate SE. (*B*) Relative YFP mRNA levels in Q44, *gcy-8*;*Q44* and *ttx-3*;*Q44* day 3 animals as determined by qRT-PCR. The values are normalized to Q44. Actin mRNA was used as an internal control. Error bars indicate SD. (*C*) Q44::YFP and tubulin levels in Q44, *gcy-8*;*Q44* and *ttx-3*;*Q44* as determined by Western analysis. Q44::YFP was detected by using the anti-GFP IR 800; tubulin was detected by using a mouse α-tubulin primary and an α-mouse IR 680 secondary antibody. The Western blot shows an overlay of signals obtained at 700 and 800 nm using the LI-COR Odyssey fluorescent imager. Note the absence of YFP degradation products.

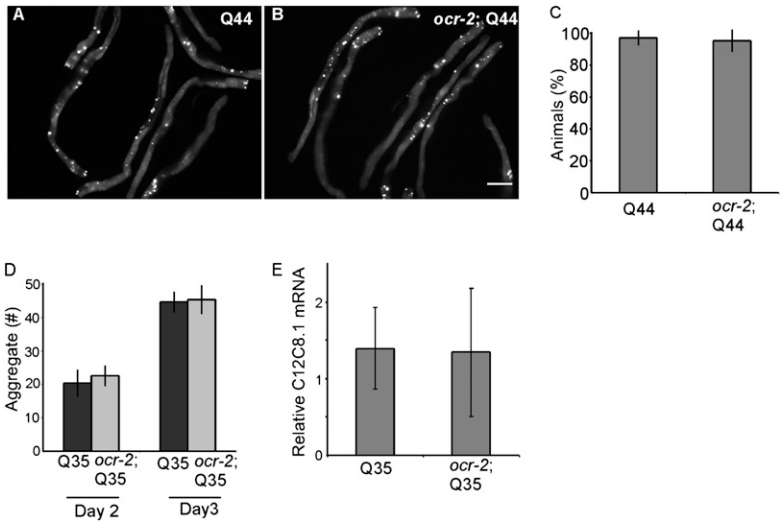

Fig. S2. Mutations affecting the chemosensory neurons do not affect the aggregation of polyQ in *C. elegans* intestinal and muscle cells. Images of Q44 (*A*) and *ocr-2*; Q44 (*B*) day 3 adult animals showing the accumulation of aggregates in the intestine. (*C*) Percentage of Q44, and *ocr-2*; Q44 day 3 adult animals that contain aggregates. Error bars indicate SE. (*D*) The average number of aggregates per animal in Q35, and *ocr-2*;Q35 in day 2 and 3 adult animals. (*E*) mRNA levels of *hsp70* (C12C8.1) in day 3 adult *Q35* and *ocr-2*;Q35 animals normalized to WT animals not expressing polyQ. Actin mRNA was used as an internal control. Error bars indicate SD.

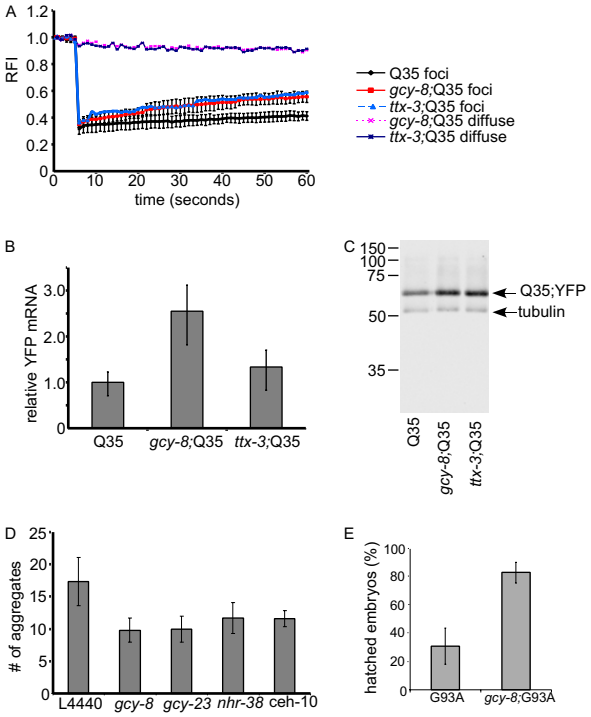

Fig. S3. Thermosensory mutant animals suppress the aggregation and toxicity caused by the expression of aggregation prone proteins in their body wall muscle cells. (*A*) FRAP measurements on 10 fluorescent foci in WT Q35, *gcy-8*;Q35 and *ttx-3*;Q35 day 3 adult animals confirmed the presence of immobile aggregates. FRAP analysis in regions of the *gcy-8*;*Q35* and *ttx-3*;*Q35* muscle cells that did not contain fluorescent foci confirmed that these regions corresponded to freely diffusing Q35::YFP. Error bars indicate SD. (*B*) Relative YFP mRNA levels in Q35, *gcy-8*;*Q35*, and *ttx-3*;*Q35* day 3 adult animals as determined by qRT-PCR. The values were normalized to Q35. Actin mRNA was used as an internal control. Error bars indicate SD. (*C*) Q35::YFP and tubulin levels in Q35, *gcy-8*;*Q35*, and *ttx-3*;*Q35* as determined by Western analysis. Q35::YFP was detected by using the anti-GFP IR 800; tubulin was detected by using a mouse α-tubulin primary and an α-mouse IR 680 secondary antibody. The Western blot shows an overlay of signals obtained at 700 and 800 nm by using the LI-COR Odyssey fluorescent imager. Note the absence of YFP degradation products. (*D*) The number of Q35 aggregates in body wall muscle cells of day 3 adult *rrf-3*;Q35 animals sensitive to neuronal RNAi, on control L4440 RNAi, and following the RNAi-induced knockdown of genes affecting thermosensory activity. The *rrf-3* background has been implicated in transgene silencing, and less Q35::YFP is expressed, and the animals accumulate fewer aggregates. (*E*) The percentage of SOD^{G93A} animals that matured beyond L2 stage at 25 °C in animals with WT thermosensory neurons, and the *gcy-8* mutant animals.

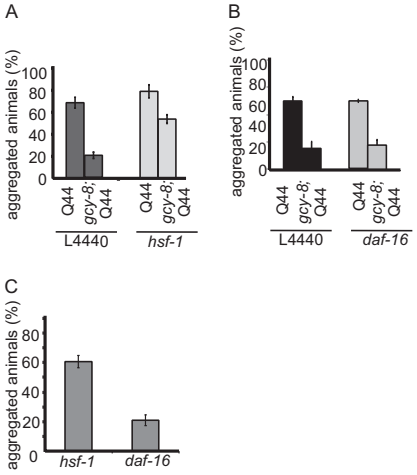

Fig. S4. Suppression of aggregation in the neuronal mutants is dependent on HSF-1 and not DAF-16. Number of animals that accumulate Q44 aggregates in WT and *gcy-8* animals grown on control bacteria (L4440) and upon RNAi-induced knockdown of (*A*) *hsf-1* or (*B*) *daf-16*. Animals scored as 3-d adults. (*C*) Percentage of animals with visible aggregates in day 3 adult *unc-31*;Q44 animals following RNAi-induced knockdown of *hsf-1* and *daf-16*. Error bars indicate SE.

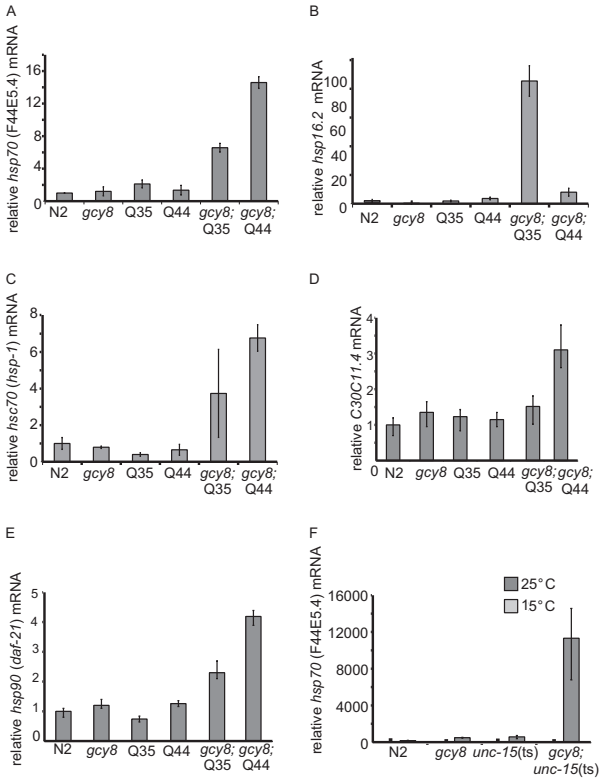

Fig. S5. Thermosensory mutants rescue proteotoxicity by enhancing protein-folding homeostasis. mRNA levels of (*A*) *hsp70* (F44E5.4), (*B*) small HSP (*hsp16.2*) and (*C*) HSC70 (*hsp-1*), (*D*) *hsp70* (C30C11.4), and (*E*) *hsp9* (*daf-21*) quantified by qRT-PCR in day 3 WT and *gcy-8* adult animals with and without the expression of polyQ. (*F*) mRNA levels of *hsp70* (F44E5.4) in WT and *gcy-8* animals in the presence and absence of the *unc-15*(ts) mutation before (15 °C) and 2 d following the misfolding of paramyosin at 25 °C, quantified by qRT-PCR. Values at 15 °C are 0.8 to 1.3, 1 to 3, 1.5 to 2.0, and 1.3 to 1.9 for WT, *gcy-8*, *unc-15*(ts), and *gcy-8*; *unc-15*(ts), respectively. All values were normalized to WT. Actin mRNA was used as an internal control. Error bars indicate SD.

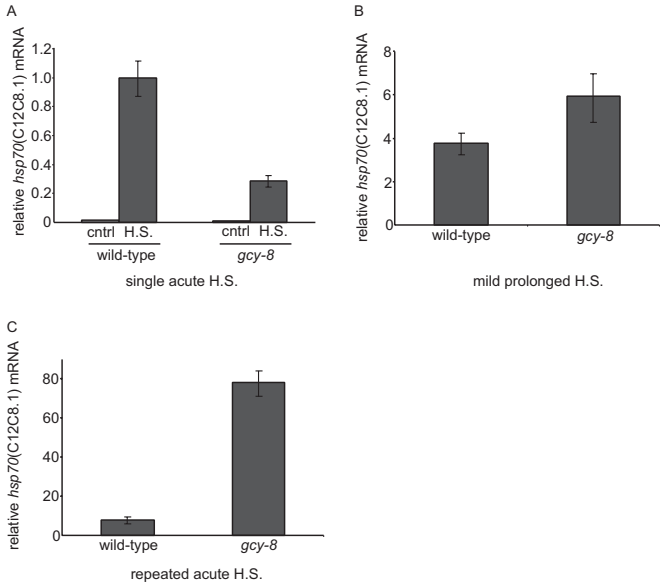

Fig. S6. Thermosensory neurons distinguish between acute HS and chronic misfolding. (*A*) relative mRNA levels of *hsp70* (C12C8.1) quantified by qRT-PCR of day 1 adult in WT and *gcy-8* mutant animals before and after a short acute HS of 34 °C for 15 min. (*B*) relative mRNA levels of *hsp70* (C12C8.1) quantified by qRT-PCR of day 1 adult WT and *gcy-8* mutant animals following prolonged, 24-h exposure to 28 °C HS of 34 °C for 15 min. Values were normalized to WT levels upon single short HS. (*C*) relative mRNA levels of *hsp70* (C12C8.1) quantified by qRT-PCR of day 1 adult WT and *gcy-8* mutant animals following repeated acute stress administered through a regimen of three exposures to 34 °C for 15 min, interspersed by 15 min recovery at 20 °C. Values were normalized to WT levels upon single short HS. Actin was used as an internal control. Error bars indicate SD.

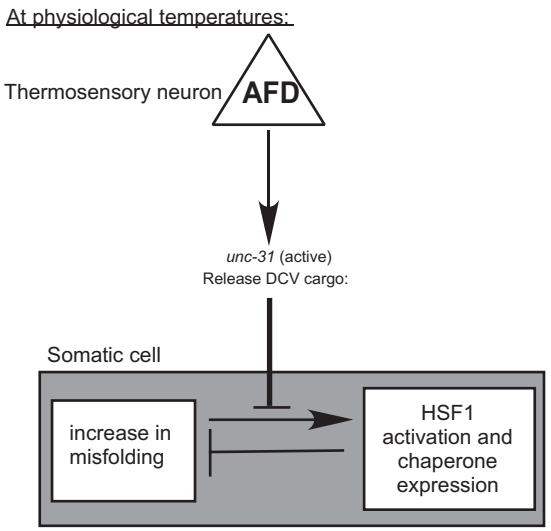

Fig. S7. Schematic of neuronal control of proteostasis. At physiological temperatures, the WT AFD thermosensory neuron exerts a net inhibitory effect on the cellular response to protein misfolding and aggregation. The suppression of chaperone up-regulation upon chronic protein misfolding in peripheral tissue, by the AFD thermosensory neuron, is accomplished through calcium-dependent DCV neurosecretion.

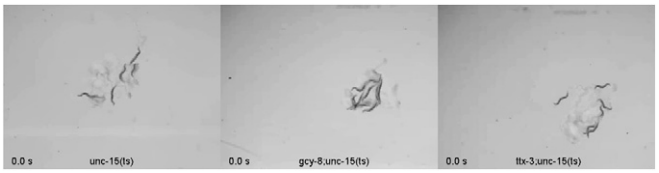

Movie S1. Thermosensory mutations suppress the toxicity caused by the misfolding of paramyosin in *unc-15* (ts) animals. The motility of *unc-15*(ts), *gcy-8;unc-15*(ts), and *ttx-3;unc-15*(ts) relative to WT animals 2 d after being transferred from 15 °C to 25 °C recorded at 5 frames/s, over the duration of 1 min. The movie is sped up by a factor of four. The phenotype of each strain is indicated.

Movie S1